NANO LETTERS

Subscriber access provided by - Access paid by the | UC Davis Libraries

Letter

Ultrasmooth Silver Thin Films Deposited with a Germanium Nucleation Layer

Logeeswaran VJ, Nobuhiko P. Kobayashi, M. Saif Islam, Wei Wu, Pratik Chaturvedi, Nicholas X. Fang, Shih Yuan Wang, and R. Stanley Williams

Nano Lett., **2009**, 9 (1), 178-182 • DOI: 10.1021/nl8027476 • Publication Date (Web): 23 December 2008

Downloaded from http://pubs.acs.org on January 15, 2009

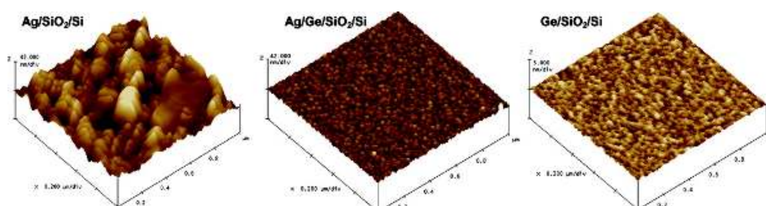

More About This Article

Additional resources and features associated with this article are available within the HTML version:

- Supporting Information
- Access to high resolution figures
- Links to articles and content related to this article
- Copyright permission to reproduce figures and/or text from this article

View the Full Text HTML

ACS Publications
High quality. High impact.

Nano Letters is published by the American Chemical Society. 1155 Sixteenth Street N.W., Washington, DC 20036

NANO LETTERS

2009
Vol. 9, No. 1
178-182

Ultrasmooth Silver Thin Films Deposited with a Germanium Nucleation Layer

Logeeswaran VJ,[†] Nobuhiko P. Kobayashi,[‡] M. Saif Islam,[*,†] Wei Wu,[§] Pratik Chaturvedi,[||] Nicholas X. Fang,[||] Shih Yuan Wang,[§] and R. Stanley Williams[§]

Department of Electrical & Computer Engineering, Kemper Hall, University of California at Davis, One Shields Avenue, Davis, California 95616, Jack Baskin School of Engineering, University of California at Santa Cruz, Santa Cruz, California 95064, Nanostructured Energy Conversion Technology and Research (NECTAR), Advanced Studies Laboratories, University of California at Santa Cruz, Santa Cruz, California 95064, NASA Ames Research Center, Moffett Field, California 94035, Information and Quantum Systems Laboratories, Hewlett-Packard Laboratories, 1501 Page Mill Road, Palo Alto, California 94304, and Department of Mechanical Science & Engineering, University of Illinois, Urbana−Champaign, 1206 West Green Street, Urbana, Illinois 61801

Received September 10, 2008; Revised Manuscript Received November 26, 2008

ABSTRACT

We demonstrate an effective method for depositing smooth silver (Ag) films on SiO_2/Si(100) substrates using a thin seed layer of evaporated germanium (Ge). The deposited Ag films exhibit smaller root-mean-square surface roughness, narrower peak-to-valley surface topological height distribution, smaller grain-size distribution, and smaller sheet resistance in comparison to those of Ag films directly deposited on SiO_2/Si(100) substrates. Optically thin (∼10−20 nm) Ag films deposited with ∼1−2 nm Ge nucleation layers show more than an order of magnitude improvement in the surface roughness. The presence of the thin layer of Ge changes the growth kinetics (nucleation and evolution) of the electron-beam-evaporated Ag, leading to Ag films with smooth surface morphology and high electrical conductivity. The demonstrated Ag thin films are very promising for large-scale applications as molecular anchors, optical metamaterials, plasmonic devices, and several areas of nanophotonics.

Many unconventional nanoelectronic devices incorporating molecules, DNA, carbon nanotubes, or semiconductor nanowires rely on the use of noble metals such as silver (Ag), platinum (Pt), and gold (Au) for electrical probing and interfacing.[1−3] The recent demonstration of the confinement of photons in miniaturized metallic waveguides and optical nanoantennas employing surface plasmons also utilized noble metal films.[4] In the embryonic field of photonic metamaterials, especially for optical imaging far beyond the diffraction limit, Ag has been the noble metal of choice.[5−7] Other novel properties, such as artificial plasmonic response, synthetic magnetism at terahertz frequencies, and negative refractive index, have also been observed with Ag films.[8] Nearly all noble metals deposited by such techniques as thermal evaporation, ion-beam-assisted deposition, and rf/dc sputtering consistently reveal a rough surface morphology with larger grains than the size suitable for desired nanoscale building blocks and electrical interfaces.[9−11] Rough surface morphologies and high sheet resistances due to the poor wettability of silver and gold, have been observed on electrically insulating substrates,[12] which led to diminished device yields and poor optical quality, repeatability, and reliability.[8,13] Therefore, the drive to produce ultrasmooth noble metal films has been a vital prerequisite for future nanodevices and systems. In this paper, we report an effective method to deposit a smooth Ag film on SiO_2/Si(100) substrates with a Ge nucleation layer. The deposited Ag films are characterized by a significantly lower root-mean-square (rms) surface roughness, narrower peak-to-valley surface topological height distribution, smaller grain-size distribution, and lower sheet electrical resistance when compared to those of Ag films deposited without a Ge nucleation layer.

The Ge and Ag depositions were done sequentially on a silicon substrate without breaking vacuum in a CHA Mark-

* Corresponding author: tel, 530-754-6732; fax, 530-752-8428; e-mail, sislam@ucdavis.edu.

[†] Department of Electrical & Computer Engineering, Kemper Hall, University of California at Davis.

[‡] Jack Baskin School of Engineering and Nanostructured Energy Conversion Technology and Research (NECTAR), Advanced Studies Laboratories, University of California at Santa Cruz and NASA Ames Research Center.

[§] Information and Quantum Systems Laboratories, Hewlett-Packard Laboratories.

[||] Department of Mechanical Science & Engineering, University of Illinois, Urbana−Champaign.

10.1021/nl8027476 CCC: $40.75 © 2009 American Chemical Society
Published on Web 12/23/2008

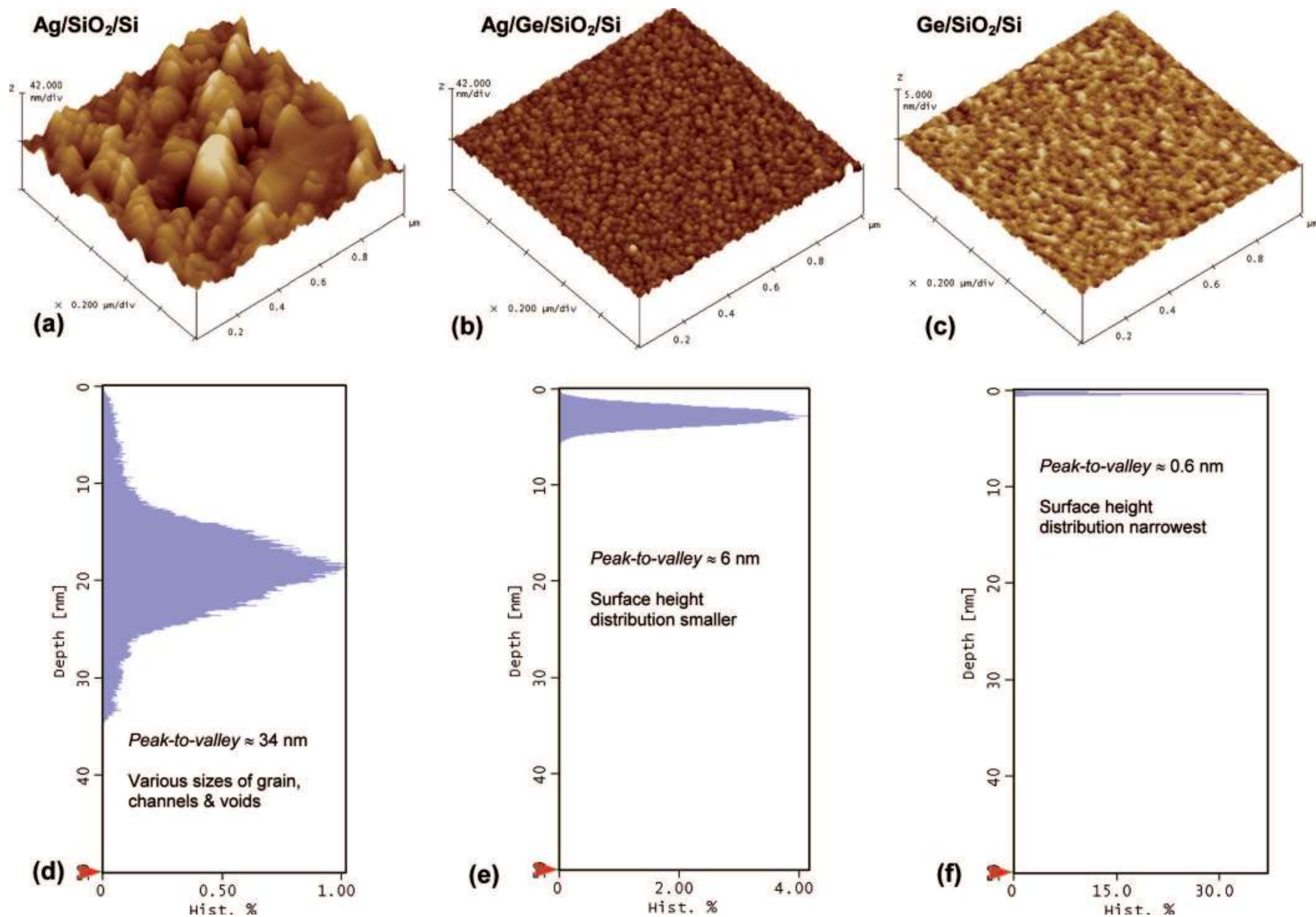

Figure 1. Representative morphologies from AFM topographs: (a) 15 nm Ag film on SiO_2/Si(100), (b) 15 nm Ag film with a 2 nm Ge overlayer on SiO_2/Si(100), and (c) 2 nm Ge on SiO_2/Si(100). (d−f) Histograms of the 2D surface-height values from the respective topographs. The surface of the Ag/SiO_2/Si sample had an rms roughness of 6−8 nm, which was an order of magnitude larger than that for the Ag/Ge/SiO_2/Si. The 2 nm seed layer of Ge on SiO_2/Si had an rms roughness of ∼0.1 nm and the rms roughness of SiO_2 is <0.1 nm. The 1 μm × 1 μm topographs (512 × 512 pixels) were plane fitted automatically to compensate for any sample tilt, and a 42 nm color scale was used to represent the height distribution for (a) and (b), while a 5 nm color scale was used for (c). The *Z* axes for the height histograms were scaled relative to the peak height.

50 ISS E-beam evaporator at a base pressure of ∼1 μTorr and at ambient temperature. Prior to the deposition, the substrate was cleaned in a "Piranha" solution of composition H_2SO_4:H_2O_2 (3:1) and dried with nitrogen. A native oxide layer (∼2−4 nm thick) was found to be present on the substrate before film deposition, and thus the substrate is referred to as SiO_2/Si(100). The deposition rate was 0.01 nm/s for Ge and 0.1 nm/s for Ag.

Thin Ag films with a nominal thickness between 10 and 20 nm were deposited on the SiO_2/Si(100) substrates covered by a Ge nucleation layer of various thicknesses (0.5, 1.0, 2.0, 5.0, 7.5, and 15 nm) for surface morphology characterization. In addition, resistors for four-point sheet resistance measurement were separately fabricated on thermally grown 100 nm SiO_2/Si(100) substrates by depositing Ag films (nominal thicknesses ∼10 nm), with and without a 1−2 nm Ge nucleation layer, in order to evaluate the influence of surface morphology on electrical resistivity. Electrical access to the resistors was made by having four contact pads patterned on each resistor by a conventional metal lift-off process with 250 nm thick Ag.[14] No further postprocessing (e.g., thermal annealing) was carried out on the blanket coated and resistor samples. The sheet resistivity was measured using a coaxial four-point probe technique with a semiconductor parameter analyzer (HP 4155B) operated in a differential voltage mode. During the probing, the current was limited to 1 mA to minimize any resistance variation due to Joule self-heating.

The surface morphology of the prepared samples was observed at room temperature using a Digital Instruments multimode atomic force microscope (AFM) in a noncontact mode at ambient conditions over a scan size of 1 μm × 1 μm and at a scan rate of 1 Hz. The collected AFM topographs were characterized quantitatively and statistically by computing the rms roughness, the peak-to-valley height difference and the grain size distribution from the topology data. Grazing incidence X-ray reflection (GIXR) measurements were used to provide an independent estimate of surface−interface roughness and thin film thickness. The GIXR data were acquired under a specular reflection geometry with the incidence angle from the surface plane varied from 0.5 to 2.5° using collimated Cu Kα (40 kV, 45 mA) X-rays as the radiation source.

Panels a and b of Figure 1 show the representative AFM images and height histograms of the Ag/SiO_2/Si(100) and

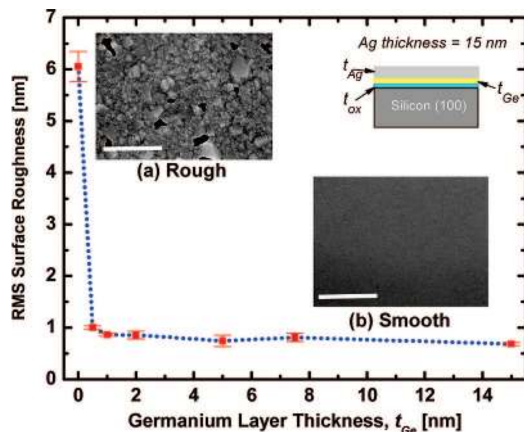

Figure 2. Plot showing the average rms surface roughness as a function of the Ge thickness for a constant Ag thickness of 15 nm (line drawn for clarity). The total improvement in surface roughness was a factor of 10, with nearly all of the improvement coming with the first 0.5 nm of Ge that was deposited. The insets (a) and (b) show the contrast between a rough and a smooth surface for SEM images of without and with Ge (scale bar is 0.5 μm).

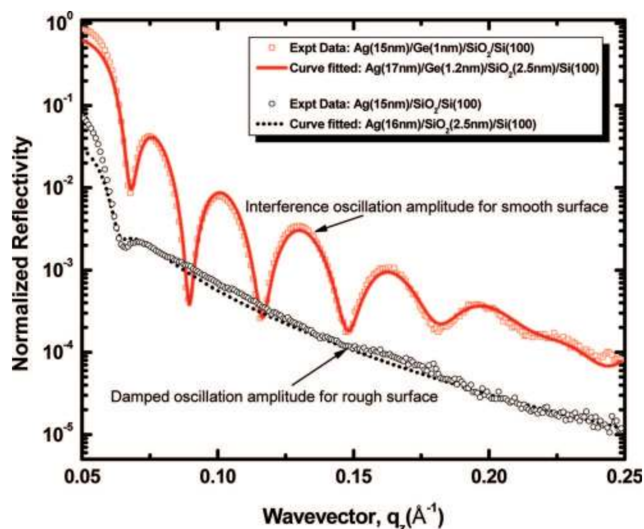

Figure 3. GIXR data (reflected intensity as a function of the surface normal component of the X-ray wavevector, q_z) for 15 nm of Ag and 1 nm of Ge on the SiO_2/Si(100) system and 15 nm of Ag on SiO_2/Si(100), clearly showing the significant difference in film uniformity of the two samples. The silicon substrate had ∼2−4 nm of native oxide. The rapid damping of the interference oscillations arises as the rms roughness becomes large. The fitted parameters are shown in the legend (error <5%).

Ag/Ge/SiO_2/Si(100) samples, respectively, while Figure 1c displays the surface morphology of evaporated Ge on the SiO_2/Si(100) substrate shown as a reference. As shown in Figure 1a, the Ag/SiO_2/Si(100) sample is rough with an average rms roughness of ∼6 nm within 1 μm^2. In addition, the average peak-to-valley height of the large grains on the Ag surface was measured to be ∼20 nm, with a high density of grain clusters of with lateral size ∼100 nm and above. Figure 1b depicts an AFM image collected on the Ag/Ge/SiO_2/Si(100) sample. The surface morphology was much smoother than that shown in the panel a, demonstrating that the presence of a thin Ge layer reduced the rms roughness (R_{rms}) of the film by at least a factor of ∼10 in comparison

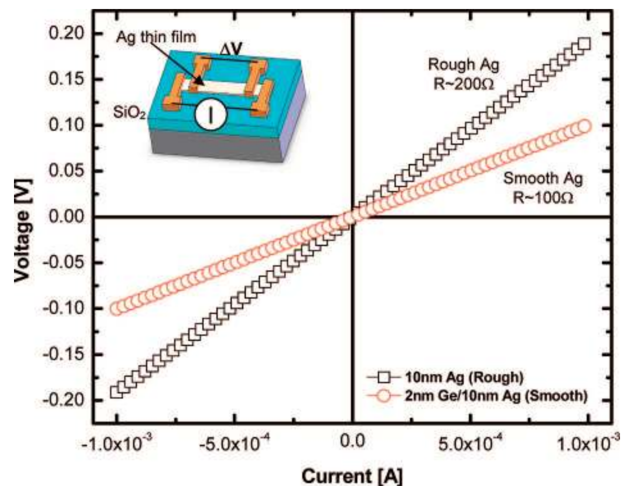

Figure 4. Representative current−voltage ($I-V$) plots for rough silver (10 nm of Ag on 100 nm of SiO_2) and smooth silver (10 nm of Ag/2 nm of Ge on 100 nm of SiO_2) films. The measured resistance of the rough silver film is ∼2× larger than the smooth silver films, with the extracted resistivities $\rho_{smooth\text{-}Ag}$ ∼20 $\mu\Omega$·cm and $\rho_{rough\text{-}Ag}$ ∼40 $\mu\Omega$·cm. Inset: schematic of the four-point sheet resistance test structure.

to thin Ag films deposited by standard techniques.[9,11,15,16] Panels d−f of Figure 1 are histograms of the two-dimensional (2D) surface-height values of the representative images shown in panels a−c of Figure 1 scaled to the peak height data. The histogram provides a measure of the maximum peak-to-valley height difference and the deviation from the average height.[17] The evaporated Ge reference film shown in Figure 1f has a fairly smooth surface (peak-to-valley height of only ∼0.6 nm). The Ag on Ge film has a narrow and symmetric height distribution, shown in Figure 1e, with a peak-to-valley height difference of ∼6 nm. The Ag film with no Ge layer in Figure 1d is characterized by two distinct height distributions, one with a total peak-to-valley difference of ∼34 nm and a narrower but more heavily populated distribution with a total height difference of ∼19 nm.

Figure 2 shows the average rms surface roughness of a set of Ag/Ge/SiO_2/Si(100) samples having a 15 nm thick Ag film deposited onto substrates with Ge layers of various thicknesses. Shown in the inset are scanning electron microscope (SEM) images that clearly show the differences in the surface morphology. A dramatic improvement in the Ag rms surface roughness from ∼6 nm to ∼1 nm was obtained for the first 0.5 nm of Ge deposited, after which the rms roughness quickly saturated at ∼0.6 nm with increasing Ge thickness.

The surface roughness averaged over a much larger scale (1 cm × 1 cm) for each sample was measured by grazing incidence X-ray reflectivity (GIXR) measurements, as shown in Figure 3. The GIXR angular plots for the 15 nm Ag/1 nm Ge on SiO_2/Si(100) sample and the 15 nm Ag on SiO_2/Si(100) sample exhibit significant differences. Persistent oscillations in the angular dependence of the scattered X-ray intensity, which result from the coherent scattering of the X-rays from the Ag surface and Ag/substrate interface, of the *Ag/Ge/SiO_2/Si(100)* sample show that this film is significantly more uniform, even at a centimeter scale, than

Table 1. Summary of Surface Morphology Parameters from AFM Image Analyses

parameter	$Ag/Ge/SiO_2/Si$ (100)	$Ag/SiO_2/Si$ (100)	$Ge/SiO_2/Si$ (100)
rms roughness, R_{rms}	~0.6−0.8 nm	~6−8 nm	~0.1 nm
peak-to-valley	~6 nm	~34 nm	~0.6 nm
grain size	~10−15 nm	~80−100 nm	<5nm
sheet resistance, $R_{\square}$	20 Ω/□	40 Ω/□	

that of the $Ag/SiO_2/Si(100)$ sample. The film thickness variation can be determined by fitting the decay in the oscillation amplitude (i.e., fast damping is caused by a rough film). As the incidence angle increases, the oscillation intensity decreases to the background noise level for both samples. The two angular distributions were analyzed using the software package Parrat32,[18] and the fitting parameters are shown in the legend of Figure 3.

The smoother Ag thin films also had a lower electrical sheet resistance. Figure 4 shows current−voltage ($I-V$) characteristics for rough Ag (10 nm) and smooth Ag (10 nm of Ag/2 nm of Ge) thin film resistors with length, $L = 500\ \mu m$ and width, $W = 100\ \mu m$ ($L/W = 5$). On the basis of the measured resistance, $R = R_{\square}\ (L/W)$, the extracted sheet resistance ($R_{\square}$, in units of ohms/square, Ω/□) for the smooth Ag film was $R_{\square,smooth-Ag}$ ~20Ω/□, a factor of 2 lower than that of the rough Ag film with $R_{\square,rough-Ag}$ ~ 40 Ω/□. The contribution of the 2 nm Ge layer to the sheet resistance was negligible.[19] The corresponding resistivity, assuming a uniform cross section for both deposited films, is $\rho_{smooth-Ag}$ ~20 $\mu\Omega \cdot cm$ and $\rho_{rough-Ag}$ ~40 $\mu\Omega \cdot cm$, which are ~13× and 26×, respectively, greater than the bulk resistivity of typical polycrystalline Ag, $\rho_0 = 1.5\ \mu\Omega \cdot cm$.[9,20] According to the Fuch−Sondheimer−Mayadas scattering theory,[21] the resistivity of a nonideal film can be expressed as $\rho = \rho_0 + \rho_{GB} + \rho_{SS} + \rho_{SR}$, where the contributions of grain-boundary (GB), surface scattering (SS), and surface roughness (SR) are added to the bulk resistivity value. From the film structure analyses (Table 1), the average grain width of the rough Ag film is 5−10 times larger than for the smooth film, and thus one would expect that grain boundary scattering should contribute much more to the measured resistivity of the smooth film than to the rough film. However, this is apparently more than compensated by the film nonuniformity and the surface irregularity of the rougher film, since the film grown without Ge has a significantly higher resistance.

Comparing the topology between Figure 1a and Figure 1b, without the layer of Ge, the deposited Ag formed distinct polycrystalline granular clusters with irregular shapes and a significant density of pinholes and voids (incomplete coalescence), which made the film electrically discontinuous. This indicates that the initial stage of Ag growth on a SiO_2/Si (100) substrate began by nucleation of isolated Ag clusters, after which the islands grew by accumulation of Ag atoms via surface diffusion[22] and coalescence into larger three-dimensional clusters (Volmer−Weber growth mode).[15,16] This resulted in a Ag film with a rough surface, characterized by a large peak-to-valley height difference, grain size, and sheet resistance.

Although the Ge film deposition on the $SiO_2/Si(100)$ substrate also occurred via Volmer−Weber growth mode,[23] the density of Ge nuclei was much larger and the islands were significantly smaller than those for Ag deposited directly on the substrate, resulting in an effectively smooth surface topology. This surface then acted as a much higher energy substrate with an elevated density of heterogeneous nucleation sites for the deposited silver atoms, which could only diffuse a few tenths of a nanometer, and thus formed a dense columnar continuous Ag film with slightly rounded caps. This growth mode resulted in a Ag film with a smoother surface, a higher grain boundary density,[24] and lower electrical sheet resistance.

This scenario is also supported by a kinetic argument: the activation energy for Ag diffusion on a Ge surface has been determined to be ~0.45 eV[25] and on a SiO_2 surface is ~0.32 eV.[26] Therefore, having a Ge nucleation layer evaporated on the substrate prior to the deposition of Ag reduces the surface diffusion and mass transportation of Ag, which results in a smooth surface topology by dense coalescence of smaller 3D columnar crystal growth.[27−31] This diffusion limited island growth mode is also consistent with Ag deposited on crystalline Ge substrates[32−35] where similar smooth surface topology has also been observed.[36]

Our previous experience showed that Ag thin films deposited onto various substrates exhibited the largest grain sizes and surface inhomogeneities among the noble metals. Here we demonstrate that even a very thin Ge layer on a silicon- or oxide-coated substrate promotes the nucleation of Ag and subsequent growth of dense and uniform films. This approach may provide a significant improvement for the fabrication of various nanoscale electronic and photonic devices. The method does not require postprocessing steps (e.g., annealing or polishing), can be easily integrated into conventional device fabrication processes, and may be implemented in several important areas of emerging nanoscale devices.

Acknowledgment. The authors thank Zhiyong Li, Sagi Mathai, Xuema Li, Doug Ohlberg, William Tong, and Denny Houng of Information and Quantum Systems Laboratories in Hewlett-Packard Laboratories, Palo Alto CA, David A. Horsley, Chan Mei-Lin, and Jack Skinner of UC Davis-Berkeley Sensor & Actuator Center, and A. Alec Talin from Sandia National Laboratories—Livermore for valuable discussions. The work at UC Davis was partially supported by NSF Grant #0547679 and a UC Davis research grant.

References

(1) Ushiku, Y.; Ono, H.; Iijima, T.; Ninomiya, N.; Nishiyama, A.; Iwai, H.; Hara, H. In *Technical Digest VLSI Technology Symposium*, Kyoto, Japan, 1993; p 121.

(2) Manepalli, R.; Stepniak, F.; Bidstrup-Allen, S. A.; Kohl, P. *IEEE Trans Adv. Packag.* **1999**, *22*, 4–8.
(3) Alford, T. L.; Adams, D.; Laursen, T.; Ulrich, B. M. *Appl. Phys. Lett.* **1996**, *68*, 3251–3253.
(4) Xu, Q.; Bao, J.; Capasso, F.; Whitesides, G. M. *Angew. Chem., Int. Ed.* **2006**, *45*, 3631–3635.
(5) Smith, D. R.; Padilla, W. J.; Vier, D. C.; Nemat-Nasser, S. C.; Schultz, S. *Phys. Rev. Lett.* **2000**, *84*, 4184–4187.
(6) Shelby, R. A.; Smith, D. R.; Schultz, S. *Science* **2001**, *292*, 77–79.
(7) Fang, N.; Lee, H.; Sun, C.; Zhang, X. *Science* **2005**, *308*, 534–537.
(8) Yen, T. J.; Padilla, W. J.; Fang, N.; Vier, D. C.; Smith, D. R.; Pendry, J. B.; Basov, D. N.; Zhang, X. *Science* **2004**, *303*, 1494–1496.
(9) Marechal, N.; Quesnel, E.; Pauleau, Y. *J. Vacuum Sci. Technol., A* **1994**, *12*, 707–713.
(10) Kim, H. C.; Theodore, N. D.; Alford, T. L. *J. Appl. Phys.* **2004**, *95*, 5180–5188.
(11) Islam, M. S.; Li, Z.; Chang, S. C.; Ohlberg, D. A. A.; Stewart, D. R.; Wang, S. Y.; Williams, R. S. In *Proc. IEEE Conf. Nanotechnol., 5th*; IEEE: Nagoya, Japan, 2005; Vol. 80, p 83.
(12) Lazzari, R.; Jupille, J. *Surf. Sci.* **2001**, *482*, 823–828.
(13) Dimmock, J. O. *Opt. Express* **2003**, *11*, 2397–2402.
(14) Prior to exposure and e-beam evaporation using the resistor contact layout mask, the photoresist was vacuum-baked at room temperature for ~3 h (to minimize any thermal effects on the Ag thin film) and the wafer subsequently cleaned using an oxygen-reactive-ion etching process with a power of ~60 W for ~10 s.
(15) Neddermeyer, H. *Crit. Rev. Solid State Mater. Sci.* **1990**, *16*, 309–335.
(16) Kundu, S.; Hazra, S.; Banerjee, S.; Sanyal, M. K.; Mandal, S. K.; Chaudhuri, S.; Pal, A. K. *J. Phys. D: Appl. Phys.* **1998**, *31*, L73–L77.
(17) Higo, M.; Fujita, K.; Tanaka, Y.; Mitsushio, M.; Yoshidome, T. *Appl. Surf. Sci.* **2006**, *252*, 5083–5099.
(18) Braun, C. *Parrat32 Software for Reflectivity*; HMI, Berlin, 1999.
(19) The resistance of the 2 nm Ge film is >5 MΩ and the Ag film essentially forms the conduction layer. There was also no significant diffusion of Ge into the thin Ag layer as evidenced by the distinct abrupt interface in the GIXR results.
(20) Gergen, B.; Nienhaus, H.; Weinberg, W. H.; McFarlanda, E. M. *J. Vac. Sci. Technol., B* **2000**, *18*, 2401–2405.
(21) Wissmann, P.; Finzel, H.-U. *Electrical Resistivity of Thin Metal Films*; Springer-Verlag: Berlin and Heidelberg, 2007.
(22) McBrayer, J. D.; Swanson, R. M.; Sigmon, T. W. *J. Electrochem. Soc.* **1986**, *133*, 1242–1246.
(23) Karmous, A.; Berbezier, I.; Ronda, A. *Phys. Rev. B* **2006**, *73*, 075323.
(24) Zhang, Z. Y.; Lagally, M. G. *Science* **1997**, *276*, 377–383.
(25) Seebauer, E. G.; Allen, C. E. *Prog. Surf. Sci.* **1995**, *49*, 265–330.
(26) Kim, H. C.; Alford, T. L.; Allee, D. R. *Appl. Phys. Lett.* **2002**, *81*, 4287–4289.
(27) Vossen, J. L. In *Physics of Thin Films*; Haas, G., Francombe, M. H., Hoffman, R. W., Eds.; Academic Press: Cleveland, OH, 1977; Vol. 9, pp 1−64.
(28) Chaurasia, H. K.; Voss, W. A. G. *Nature* **1974**, *249*, 28–29.
(29) Arbab, M. *Thin Solid Films* **2001**, *381*, 15–21.
(30) Anders, A.; Byon, E.; Kim, D. H.; Fukuda, K.; Lim, S. H. N. *Solid State Commun.* **2006**, *140*, 225–229.
(31) Allara, D. L.; Hebard, A. F.; Padden, F. J.; Nuzzo, R. G.; Falcone, D. R. *J. Vac. Sci. Technol., A* **1983**, *1*, 376–382.
(32) Rossi, G.; Abbati, I.; Braicovich, L.; Lindau, I.; Spicer, W. E. *Phys. Rev. B* **1982**, *25*, 3619–3626.
(33) Nakatsuji, K.; Takagi, Y.; Yamada, M.; Naitoh, Y.; Komori, F. *Surf. Sci.* **2005**, *591*, 108–116.
(34) Miller, T.; Rosenwinkel, E.; Chiang, T. C. *Phys. Rev. B* **1984**, *30*, 570–577.
(35) Jonas, K. L.; Von Oeynhausen, V.; Bansmann, J.; Meiwes-Broer, K. H. *Appl. Phys. A: Mater. Sci. Process.* **2006**, *82*, 131–137.
(36) Basile, L.; Hong, H. W.; Czoschke, P.; Chiang, T. C. *Appl. Phys. Lett.* **2004**, *84*, 4995–4997.

NL8027476